Computer simulation of ultrawideband Vivaldi active phased array antenna*

Yurii Palianytsia[1,*,†], Vasyl Dunets[1,†], Grygorij Khymych[1,†], Oleg Zastavnyy[2,†] and Alexander Los[3,†]

[1] Ternopil Ivan Pului National Technical University, Rus'ka St, 56, Ternopil, Ukraine
2 West Ukrainian National University, Lvivska str. 11, Ternopil, 46009, Ukraine
3 Central Research Institute of the Armed Forces of Ukraine

Abstract

The utilization of computer simulation in technology development, exemplified by the ultrawideband Vivaldi active phased array antenna instead of omnidirectional antennas for ecological monitoring and drone video broadcasting, offers a multitude of advantages. These include substantial cost savings, enhanced environmental sustainability, and an improved ability to control experimental conditions. By adopting computer simulation, we can minimize health risks and environmental impacts, making it a safer and more efficient approach for societal well-being and a greener future.

Keywords

computer simulation, ultrawideband Vivaldi antenna, active phased array antenna, ecological monitoring, drone, video broadcasting

1. Introduction

Ecological monitoring has become increasingly important due to the growing environmental concerns, such as climate change, deforestation, pollution, and wildlife conservation. Traditional methods of ecological monitoring have limitations, including high costs, time constraints, safety risks, and accessibility issues. In recent years, unmanned aerial vehicles (UAVs), also known as drones, have emerged as powerful tools for ecological monitoring owing to their versatility, speed, accuracy, and cost-effectiveness. Drones have emerged as a powerful tool for ecological monitoring, offering unprecedented flexibility, detail, and accessibility. The state-of-the-art in this field continues to advance rapidly, driven by technological innovations and a growing recognition of the potential benefits to conservation efforts. By leveraging the unique capabilities of drones and combining them with advanced data analysis techniques, scientists can gain valuable insights into ecosystem dynamics and inform effective conservation strategies [1].

In the context of drone video broadcasting, the frequency bands of 1.2, 2.4, 5.6 and 5.8 GHz are commonly utilized. These bands are chosen for their ability to offer higher available bandwidths, which is critical for transmitting video images with minimal interference. The 2.4 GHz and 5.8 GHz bands, in particular, are widely used due to their compatibility with many commercial drones. A study on Real-Time Video Transmission and Communication System via Drones over long distances found that frequencies around 2.2 and 2.3 GHz provided the best video-reception time, which is less than 100 seconds [2]. This suggests that the lower end of the 2.4 GHz band is optimal for real-time video transmission. The chapter Drone Technology: Types, Payloads, Applications, Frequency Spectrum Issues and Future Developments discusses the importance of frequency

* CITI'2025: 3rd International Workshop on Computer Information Technologies in Industry 4.0, June 11–12, 2025, Ternopil, Ukraine
[1,*] Corresponding author.
[†] These authors contributed equally.
palanizayb@tntu.edu.ua (Y. Palianytsia); vasyadunets@gmail.com (V. Dunets); khymuch@tntu.edu.ua (G. Khymych); olegz80@gmail.com (O. Zastavnyy); BANKSYNCR@gmail.com (A. V. Los)
0000-0002-8710-953X (Y. Palianytsia); 0000-0003-2513-9191 (V. Dunets); 0000-0001-6760-5811 (G. Khymych); 0000-0001-8630-8791 (O. Zastavnyy); 0000-0002-6636-4208 (A. V. Los)

spectrum for drone communication. It mentions that two popular license-free bands used for drones for command and control and payload communications are the 2.4000-2.4835 MHz and 5.470-5.725 MHz bands, which align with the 2.4 GHz and 5.8 GHz bands commonly used in commercial drones [3].

2. Latest findings

The field of ultrawideband (UWB) Vivaldi active phased array antennas is a rapidly evolving area of research, particularly pertinent to applications in ecological monitoring and drone video broadcasting. The integration of UWB technology in Vivaldi antennas has been instrumental in enhancing the performance of communication systems by providing high directivity and gain across a wide range of frequencies.

One notable approach in this domain is presented by Jiwan Ghimire et al., who developed a compact, wideband, high-gain six-slot Vivaldi antenna array on a single substrate layer. Their design utilizes a unique combination of power splitters based on binary T-junction power splitter topology, frequency-independent phase shifter, and a T-branch, resulting in highly directive radiation patterns and optimal return losses (S-parameters) across the UWB frequency band [4].

Another significant contribution is from Ahmad Hatami, Afsaneh Saee Arezomand, and Ferdows B. Zarrabi, who reviewed various models of Vivaldi antennas to achieve a linear or constant phase center. They emphasized the importance of controlling the field distribution around the antenna for phase control, which is crucial for radar applications and microwave sensing [5].

Furthermore, the work on balanced antipodal Vivaldi antennas for wide bandwidth phased arrays has shown promising results. These antennas are known for their good performance over a wide bandwidth, which is essential for the reliable transmission of high-quality video images from drones [6].

The advancements in UWB Vivaldi active phased array antennas are poised to significantly impact ecological monitoring by providing enhanced resolution and sensitivity for environmental data collection. As the technology continues to mature, we can expect further innovations that will solidify its role in modern communication systems.

The integration of computer simulation in the development of technologies like the ultrawideband Vivaldi active phased array antenna presents numerous benefits over traditional in vitro and in vivo experiments. These range from substantial economic savings and improved environmental sustainability to enhanced precision and control over experimental conditions. By reducing health risks and minimizing the environmental footprint, computer simulation stands as a superior alternative, fostering both scientific innovation and societal well-being.

3. Advanced mathematical aspects of PCB Vivaldi active phased array antennas

The understanding of mathematical aspects of Printed Circuit Board (PCB) Vivaldi antennas is a complex task that involves various aspects of electromagnetic theory and signal processing [7-11]. Vivaldi antennas, known for their wide bandwidth and end-fire radiation patterns, are a type of continuous transverse stub (CTS) antennas [12]. Their design is based on the exponential tapering of a slot line which results in a traveling wave antenna with a flared aperture.

3.1. Geometrical design and parameters of single antenna element

The fundamental geometry of a Vivaldi antenna can be described by an exponentially tapered slot on a dielectric substrate. The taper rate, which determines the opening of the slot, is a critical parameter that affects the antenna's impedance bandwidth and gain. The taper rate K_a can be expressed mathematically as:

$$K_a = \frac{1}{L_{taper}} \left(\log \frac{W_{taper}}{s} \right), \tag{1}$$

where L_{taper} is the length of the taper, $W_{taper}$is the width of the aperture, s is the slot line width.

3.2. Impedance Matching

For optimal performance, the antenna must be impedance matched to the transmission line. This is often achieved using a microstrip line with a specific characteristic impedance. The impedance $Z(x)$ along the tapered slot line can be modeled as a function of the position x, which varies from the feed point to the aperture.

The impedance transformation can be represented as:

$$Z(x) = Z_0 e^{K_a x}, \tag{2}$$

where Z_0 is the characteristic impedance at the feed point.

3.3. Radiation pattern and gain

The radiation pattern of a Vivaldi antenna is determined by the distribution of the electric field along the aperture. The far-field radiation pattern $E(\theta, \phi)$ in spherical coordinates can be approximated using the aperture field distribution and the taper profile. The gain G of the antenna can be calculated by integrating the radiation intensity over the entire radiation sphere:

$$G = \frac{4\pi E(\theta, \phi)_{max}}{P_{rad}}, \tag{3}$$

where P_{rad} is the total radiated power.

3.4. Signal propagation and dispersion

The signal propagation along the tapered slot line is subject to dispersion, which can be modeled using the telegrapher's equations. The phase velocity v_p and group velocity v_g are crucial for understanding the broadband characteristics of the antenna:

$$\begin{aligned} v_p &= \frac{1}{\sqrt{L' C'}}, \\ v_g &= \frac{d\omega}{dk}, \end{aligned} \tag{4}$$

where L' and C' are the per-unit-length inductance and capacitance, ω is the angular frequency, k is the wave number.

3.5. Electromagnetic wave propagation

The performance of a Vivaldi antenna is heavily influenced by the propagation of electromagnetic waves along the tapered slot. The propagation can be described by Maxwell's equations, which in the case of a Vivaldi antenna, are often simplified to the transverse electromagnetic (TEM) mode due to the planar structure of the antenna. The electric E and magnetic H fields in the TEM mode can be expressed as:

$$E(x, y, z) = -\nabla \Phi(x, y) e^{-j\beta z} \tag{5}$$

$$H(x,y,z)=\frac{1}{\eta}\hat{z}\times\nabla\Phi(x,y)e^{-j\beta z},$$

where $\Phi(x,y)$ is the electric potential, β is the propagation constant, η is the intrinsic impedance of the medium.

3.6. Antenna aperture

The aperture of the Vivaldi antenna, which is the open end of the tapered slot, acts as the radiating element. The field distribution across the aperture can be modeled using the aperture field method, which assumes that the fields in the aperture are equivalent to those on an imaginary surface in the near-field region. The aperture fields $E_{ap}(x,y)$ are related to the far-field pattern $F(\theta,\phi)$ by the Fourier transform:

$$F(\theta,\phi)=\iint_{aperture}E_{ap}(x,y)e^{-j(k_x x+k_y y)}dxdy, \tag{6}$$

where k_x and k_y are the wave vector components in the x and y directions, respectively.

3.7. Dispersion Analysis

The dispersion characteristics of the Vivaldi antenna are crucial for its wideband performance. The dispersion relation, which links the frequency f to the propagation constant β can be derived from the transmission line model of the tapered slot. For a non-dispersive line, the relation is linear; however, for a Vivaldi antenna, the relation is more complex due to the varying geometry:

$$\beta(f)=\frac{2\pi f}{v_p(f)}, \tag{7}$$

where $v_p(f)$ is the frequency-dependent phase velocity.

3.8. Numerical methods for simulation

To accurately simulate the performance of a Vivaldi antenna, numerical methods such as the Finite-Difference Time-Domain (FDTD) method or the Transmission-Line Matrix (TLM) method are employed in Matlab Antenna and RF Toolboxes. These methods discretize the antenna structure into a grid and solve Maxwell's equations iteratively over time or frequency. The simulation provides detailed information about the antenna's impedance, radiation pattern, and gain across its operating bandwidth.

3.9. Optimization techniques

Mathematical optimization build-in techniques of Matlab Antenna, RF and Phased Array System Toolboxes are used to fine-tune the design of Vivaldi antennas and arrays by default. Techniques such as genetic algorithms (GAs) or particle swarm optimization (PSO) are applied to maximize the antenna's performance metrics, such as gain or bandwidth, by adjusting design parameters like the taper rate or substrate material properties.

3.10. Array configuration and element spacing

The geometry of the phased array is defined by the placement of the individual antenna elements. For a 2x5 array, we have two rows and five columns of elements. The spacing between the elements, both inter-row and inter-column, is a critical factor that influences the array's performance. The element spacing d is a fraction of the wavelength λ to avoid grating lobes $d\le\frac{\lambda}{2}$.

3.11. Beamforming and steering

Beamforming is achieved by adjusting the phase of the signal at each antenna element. For a desired beam direction θ_0 and ϕ_0 , the phase shift $\Delta\phi_{mn}$ for the element at row m and column n is given by:

$$\Delta\phi_{mn} = \frac{2\pi}{\lambda}\left(m\,d_y \sin\left(\phi_0\right)\sin\left(\theta_0\right) + n\,d_x \cos\left(\theta_0\right)\right), \tag{8}$$

where d_x and d_y are the inter-element spacings in the x and y directions, respectively.

3.12. Impedance matching and mutual coupling

Each element in the array must be impedance matched to ensure maximum power transfer. Additionally, mutual coupling between elements must be considered, as it affects the input impedance of each element. The input impedance $Z_{(}\in, mn\big)$ of the element at position m, n can be modeled as:

$$Z_{\dot{c},mn} = Z_0 + j\,X_{mn} + \sum_{\substack{p,q \\ (p,q)\neq(m,n)}} Z_{coup,pq}, \tag{9}$$

where Z_0 is the characteristic impedance, X_{mn} is the reactance due to the element's own structure, $Z_{coup,pq}$ represents the mutual coupling impedance from the element at position p, q.

3.13. Radiation Pattern and Gain

The radiation pattern of the array is the result of the superposition of the patterns from each element. The total electric field E_{total} in the far-field can be expressed as:

$$E_{total}(\theta,\phi) = \sum_{m=1}^{M}\sum_{n=1}^{N} E_{mn}(\theta,\phi)\,e^{-j\Delta\phi_{mn}}, \tag{10}$$

where $E_{mn}(\theta,\phi)$ is the radiation pattern of the individual element at position m, n,

M and N are the number of rows and columns, respectively.

Understanding of PCB Vivaldi Antenna Arrays mathematical aspects encompasses a comprehensive analysis of their element spacing, beamforming, impedance matching, and mutual coupling, signal propagation, and dispersion. Numerical simulations play a vital role in predicting the antenna's performance and guiding the optimization process to achieve the desired wideband characteristics. Using standard-de-facto Matlab tools ensures that Vivaldi antennas can meet the stringent requirements of modern communication systems, including those used for ecological monitoring and drone video broadcasting.

4. Design and computer simulation results

4.1. Single PCB ultrawideband Vivaldi antenna element

Based on the technical requirements, our single PCB ultrawideband Vivaldi antenna element [7] is designed to cover video transmission bands of 1.2, 2.4, 5.6 and 5.8 GHz. The design of the antenna element (Figure. 1a) is executed in the form of a PCB stack (Figure. 1b), where the top side features a cooper layer on FR4 laminate, creating the board shape for the antenna. On the bottom side of the stack, within the lower copper layer, a radial stub matching circuit (commonly referred to as a "bowtie") is constructed to extract electromagnetic energy from the Vivaldi antenna element.

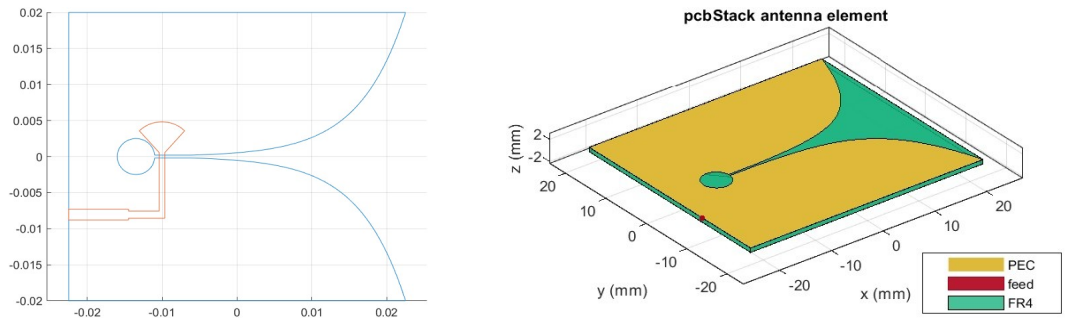

(a) (b)

Figure 1: Geometric dimensions of single Vivaldi antenna element of the active phased array antenna.

Leveraging the Matlab Integrated Development Environment , the 3D directivity pattern of the Vivaldi antenna element has been constructed in three-dimensional coordinates for 1.2, 5.4 GHz bands and for 5.6, 5.8 GHz bands, as depicted in Figure 2 and Figure 3 respectively. This graphical representation provides an insightful visualization of the antenna's radiation pattern, crucial for the precise calibration and optimization of its performance in targeted applications.

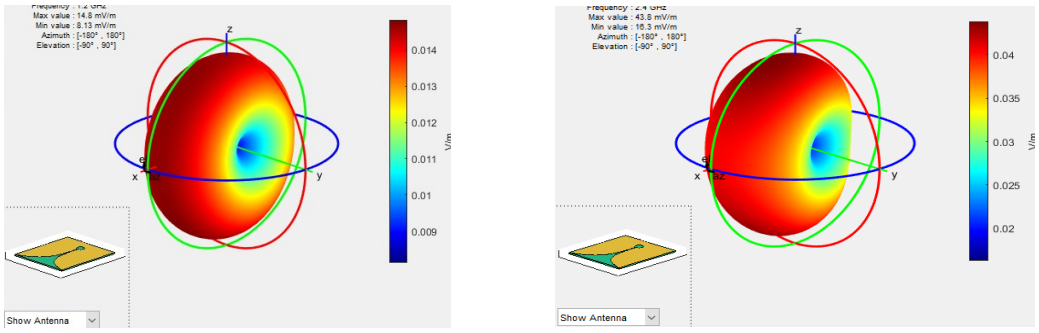

(a) (b)

Figure 2: Directivity diagram plot of Vivaldi antenna element pattern in 3-dimensional coordinates for 1.2, 2.4 GHz bands.

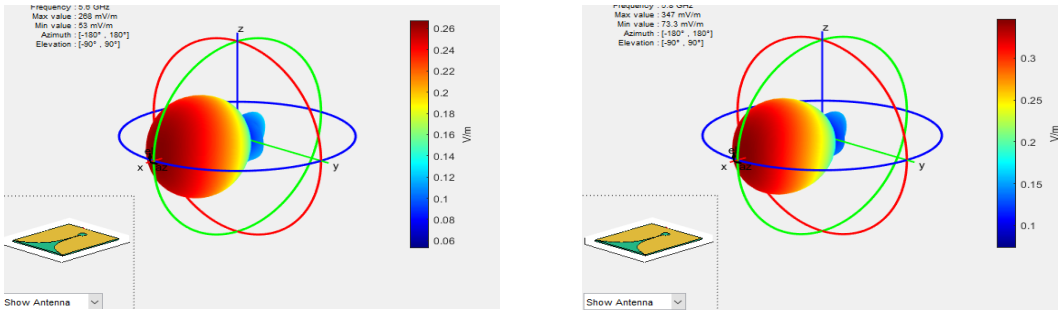

(a) (b)

Figure 3: Directivity diagram plot of Vivaldi antenna element pattern in 3-dimensional coordinates for 5.6, 5.8 GHz bands.

The directivity diagrams of the Vivaldi antenna element have been calculated for video broadcasting frequency ranges of 1.2 (a), 2.4 (b), 5.6 (c), and 5.8 GHz (d), as illustrated in Figure 4. It is observed that the directivity diagrams exhibit asymmetry, which is a characteristic inherent to Vivaldi antennas. The asymmetrical pattern of the Vivaldi antenna element will be neutralized when integrated into an antenna array, which is advantageous for targeted video broadcasting. This ensures precise transmission and reception within the designated frequency bands, optimizing the antenna's performance for specific communication needs.

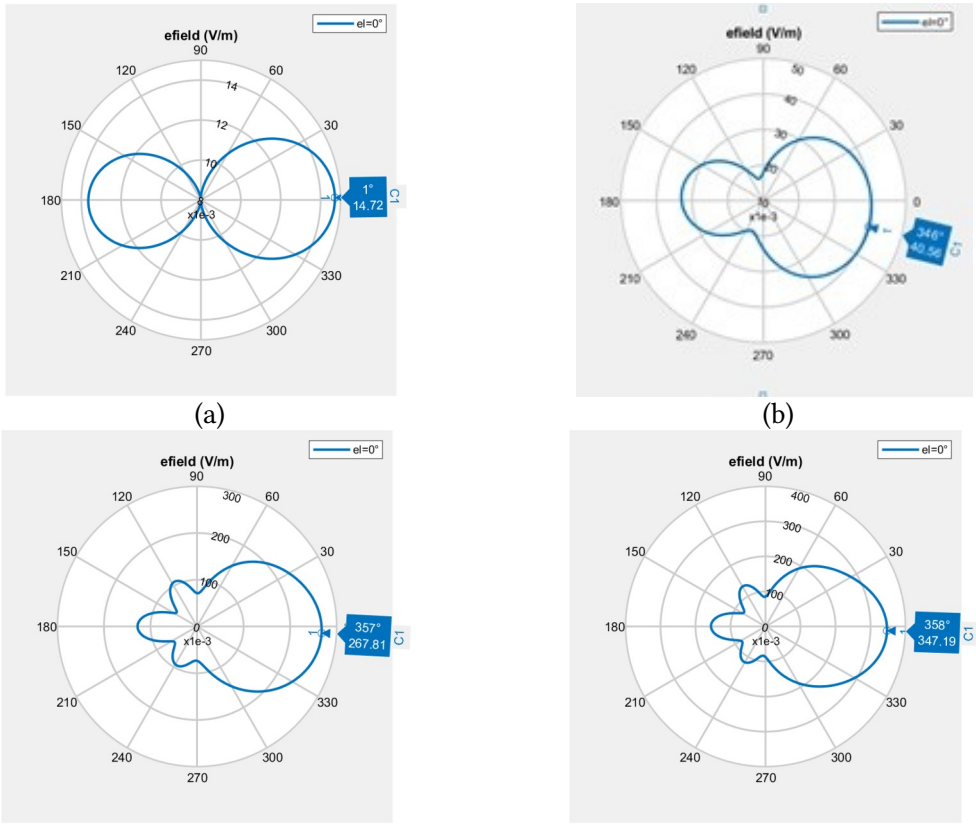

Figure 4: Directivity diagram plot of Vivaldi antenna element pattern in 2-dimensional coordinates for 5.6, 5.8 GHz bands.

It is observed that the directivity diagrams exhibit asymmetry, which is a characteristic inherent to Vivaldi antennas. The asymmetrical pattern of the Vivaldi antenna element will be neutralized when integrated into an antenna array, which is advantageous for targeted video broadcasting. This ensures precise transmission and reception within the designated frequency bands, optimizing the antenna's performance for specific communication needs.

Using the Matlab RF Toolbox, we computed the input impedance of a single Vivaldi antenna element and plotted the resistance and reactance across the specified frequencies of 1.2 GHz, 2.4 GHz, 5.6 GHz, and 5.8 GHz, respectively (Figure 5a). This analysis showed the variation in impedance with frequency, which is crucial for achieving proper impedance matching and minimizing signal reflection.

Moreover, we calculated the S-parameters for the single Vivaldi antenna element, focusing on the S_{11} parameter, which represents the input reflection coefficient. The S_{11} parameter, also known as the return loss, indicates how much power is reflected back towards the source (Figure 5b). An S_{11} value of 0 dB implies that all the power is reflected and none is radiated, which is undesirable. To achieve efficient radiation, the S_{11} value must be minimized.

The design incorporates impedance matching and mutual coupling mitigation techniques to ensure optimal performance and efficiency. Each Vivaldi element is individually matched to the characteristic impedance of the feed network, and the effects of mutual coupling between adjacent elements are minimized through careful array optimization.

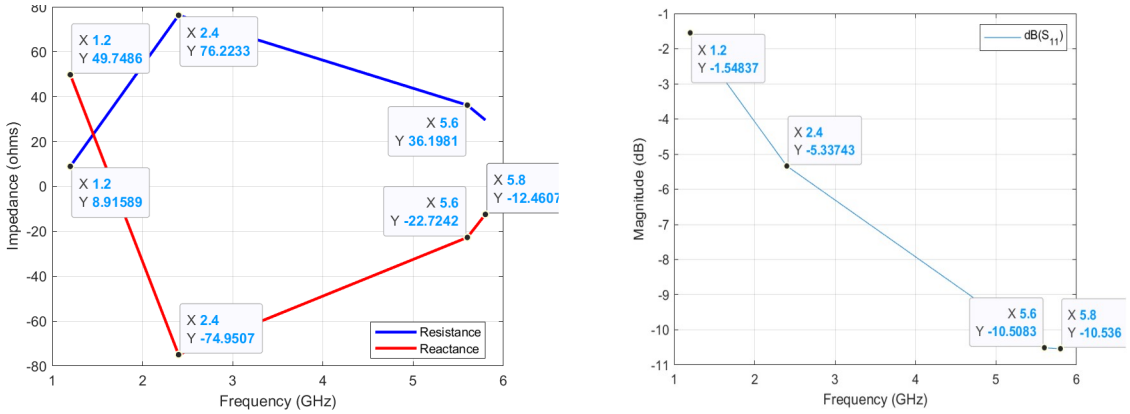

Figure 5: Input impedance (a) and reflection coefficient (S_{11}-parameter) of single Vivaldi antenna element of the active phased array antenna.

4.2. Ultrawideband Vivaldi active phased array antenna

We have constructed an active phased array antenna comprising a 2x5 configuration (2 rows horizontally by 5 columns vertically) of Vivaldi antenna elements. This arrangement enables a narrow beam pattern in the horizontal plane (azimuth), which is advantageous for our application. In our case, a high degree of resolution in the vertical plane (elevation) is not a critical requirement. The design leverages the individual Vivaldi antenna elements discussed earlier, with their optimized performance across the desired frequency bands for video broadcasting (1.2, 2.4, 5.6, and 5.8 GHz). By arranging these elements in a phased array configuration, we can achieve beamforming capabilities, allowing us to steer the radiation pattern in the desired direction electronically.

The inter-element spacing within the array is a crucial parameter that must be carefully chosen to avoid the formation of grating lobes and to ensure optimal radiation characteristics. In our design, the spacing between adjacent elements in both the horizontal and vertical directions is set to be less than half the wavelength ($d<\lambda/2$) at the central operating frequency of 2.4 GHz. This spacing ensures that the array radiates a single main beam without the presence of significant grating side lobes.

To achieve beamforming and beam steering, the signals fed to each antenna element are phase-shifted according to the desired beam direction. The phase shift required for an element located at the m-th row and n-th column (m,n) is given by the following equation:

$$\Phi_m n=2\pi/\lambda\left(m d_y \sin\left(\theta_0\right)\sin\left(\varphi_0\right)+n d_x cos\left(\theta_0\right)\right), \tag{11}$$

where d_x and $d_y$are the inter-element spacings in the, x (horizontal) and y (vertical) directions, respectively, θ_0 and $\varphi_0$are the desired elevation and azimuth angles, respectively, for the main beam direction, λ is the wavelength corresponding to the operating frequency.

By adjusting the phase shifts applied to each element, we can steer the main beam in the desired direction, enabling electronic beam scanning capabilities for the array.

The resulting ultrawideband Vivaldi active phased array antenna provides a highly directive radiation pattern that can be steered electronically, making it well-suited for applications such as ecological monitoring and drone video broadcasting. The narrow azimuthal beamwidth allows for precise directional transmission and reception, while the wideband frequency coverage accommodates the required video transmission bands.

We projected the radiation pattern of the ultrawideband Vivaldi active phased array antenna onto the terrain surface for frequencies of 1.2 GHz (Figure 6a), 2.4 GHz (Figure 6b), 5.6 GHz (Figure 6c), and 5.8 GHz (Figure 6d), respectively.

The projected radiation patterns onto the terrain surface provide valuable insights into the antenna's performance in real-world scenarios. These simulations take into account the effects of the environment, including obstacles, terrain features, and potential sources of interference along propagation.

At the lower frequencies of 1.2 GHz (Figure 6a) and 2.4 GHz (Figure 6b), the radiation patterns exhibit a broader beamwidth, which is advantageous for covering larger areas during ecological monitoring or video broadcasting missions. However, as the frequency increases to 5.6 GHz (Figure 6c) and 5.8 GHz (Figure 6d), the beamwidth becomes narrower, enabling more precise and directional transmission and reception.

The narrower beamwidth at higher frequencies is particularly beneficial for applications that require higher data rates or higher-resolution video transmission, as it minimizes interference from adjacent sources and improves the signal-to-noise ratio (SNR) at the receiver.

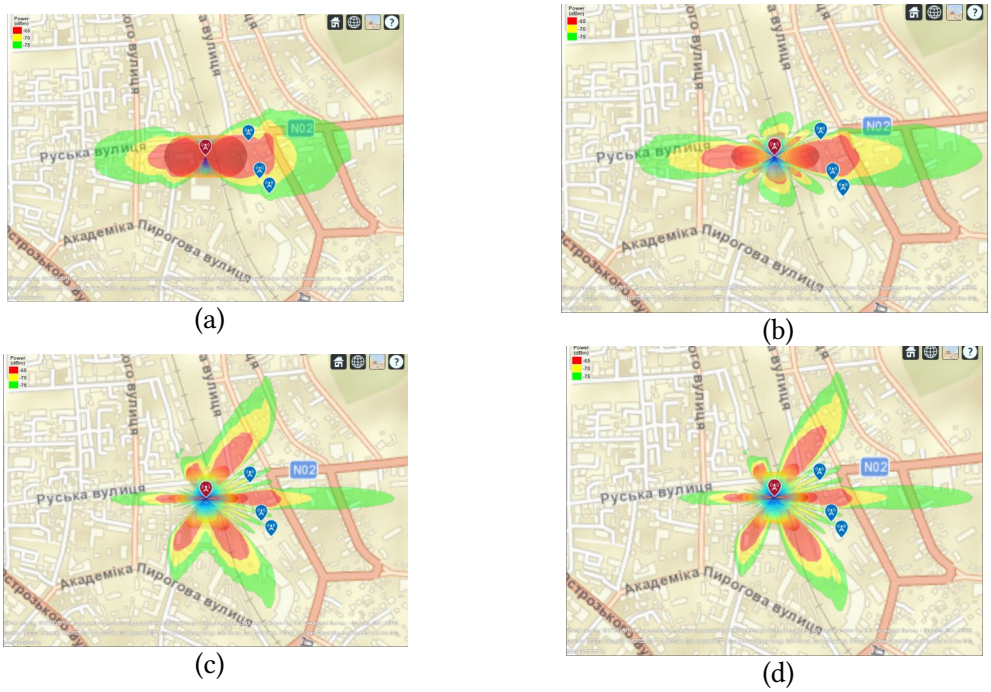

Figure 6: Radiation pattern of the ultrawideband Vivaldi active phased array antenna projected onto the terrain surface for (a) 1.2 GHz, (b) 2.4 GHz, (c) 5.8 GHz, and (d) 5.8 GHz.

It is important to note that the radiation patterns are also influenced by the antenna's gain and directivity, which can vary across the operating frequency bands (Figure 6). The simulations take these factors into account, providing an accurate representation of the antenna's performance in different environments and scenarios.

These terrain-projected radiation patterns serve as valuable tools for mission planning and optimization, allowing us to anticipate potential challenges and optimize the antenna's configuration and positioning for maximum effectiveness in ecological monitoring and drone video broadcasting applications.

In the virtual environment experiments, the received/transmitted signals sensitivities of -65 dB for strong signals, -70 dB for medium signals, and -75 dB for weak signals are accepted (see Table 1 for details). In the first column of the table, we see that the frequency bands being tested were 1.2 GHz, 2.42 GHz, 5.8 GHz, and 5.8 GHz. As frequency increased, the main beam width of the phased antenna arrays became narrower. The second column lists the communication conditions, which included three types: "freespace," where there were no obstructions present, "gas," representing air temperatures of 35°C, "fog," indicating water density of 0.5 grams per cubic meter, and "rain," signifying rainfall intensity of approximately 50 millimeters per hour. The experimental results demonstrate the feasibility and cost-effectiveness of fabricating a practical prototype based on our

designed phased antenna array. Column "Rx/Tx" denotes the numbered receivers/transmitters shown on Figure 4 (markers are numbered top to bottom). They can function as transmitter, receiver, interference source, or interference receiver simultaneously in any combination. To simplify the results table, all receivers have a sensitivity level of -75 dB. Column "SigStrength" displays the received signal strength in decibels. Lastly, column "Sens-SS" indicates the difference between the sensitivity levels (-75 dB for each receiver) and "SigStrength" for every receiver.

Table 1
The results of virtual experiment

f, GHz	Conditions	Rx/Tx	Sigstrength, dB	Sens-SS, dB
1.2	freespace	1	-51.5342307	23.4657693
1.2	freespace	2	-55.11911941	19.8808806
1.2	freespace	3	-59.83948441	15.1605156
1.2	gas	1	-51.53489369	23.4651063
1.2	gas	2	-55.11998138	19.8800186
1.2	gas	3	-59.84057389	15.1594261
1.2	rain	1	-51.53683184	23.4631682
1.2	rain	2	-55.12250144	19.8774986
1.2	rain	3	-59.84375913	15.1562409
2.4	freespace	1	-59.04922294	15.9507771
2.4	freespace	2	-68.86587616	6.13412384
2.4	freespace	3	-74.2835649	0.7164351
2.4	gas	1	-59.04988594	15.9501141
2.4	gas	2	-68.86673813	6.13326187
2.4	gas	3	-74.28465438	0.71534562
2.4	rain	1	-59.05182408	15.9481759
2.4	rain	2	-68.86925819	6.13074181
2.4	rain	3	-74.28783962	0.71216038
5.6	freespace	1	-82.70503917	7.70503917
5.6	freespace	2	-74.68484423	0.31515577
5.6	freespace	3	-97.60965464	22.6096546
5.6	gas	1	-82.70589655	7.70589655
5.6	gas	2	-74.68595891	0.31404109
5.6	gas	3	-97.61106355	22.6110635
5.6	rain	1	-82.77858988	7.77858988
5.6	rain	2	-74.78047572	0.21952428
5.6	rain	3	-97.73052804	22.730528
5.8	freespace	1	-97.13548926	22.1354893
5.8	freespace	2	-73.95533155	1.04466845
5.8	freespace	3	-83.77828778	8.77828778
5.8	gas	1	-97.13636252	22.1363625
5.8	gas	2	-73.95646688	1.04353312
5.8	gas	3	-83.77972277	8.77972277
5.8	rain	1	-97.22045878	22.2204588
5.8	rain	2	-74.06580955	0.93419045
5.8	rain	3	-83.91792639	8.91792639

The above simulation results show how the signal sensitivity varies under various environmental conditions using our proposed ultrawideband Vivaldi active phased array antenna. This data will help guide optimal placement and orientation of the antennas for specific purposes like ecological monitoring and drone video broadcasting. Additionally, it highlights the versatility and adaptability of this antenna system in diverse settings. Further research could explore ways to

further enhance its performance through modifications to the feeding network and incorporating advanced control algorithms.

For enhanced understanding, a comprehensive stepwise high-level flowchart diagram of proposed simulation approach is developed outlining each phase of the suggested simulation technique displayed in Figure 5. This more elaborate rendition provides increased insight into the intricate procedures included within the simulation procedure, making it especially helpful for understanding. Such a detailed flowchart serves as a handy reference point during the simulation process, ensuring consistency and precision in implementing the proposed simulation strategy.them.

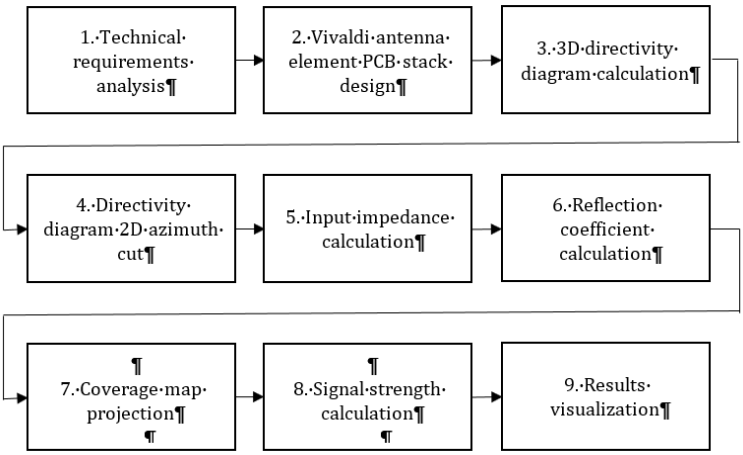

Figure 7: Stepwise high-level flowchart diagram of proposed simulation approach.

5. Discussion

The computer simulation approach employed in this study has demonstrated its effectiveness in designing and optimizing an ultrawideband Vivaldi active phased array antenna for ecological monitoring and drone video broadcasting applications. However, it is essential to acknowledge and discuss the potential limitations and challenges associated with this approach, as well as explore future research directions to further enhance the applicability and performance of the proposed antenna system.

One of the primary limitations of computer simulations is their reliance on accurate modeling and approximations. While sophisticated computational techniques and advanced simulation tools have been utilized in this study, there may still be discrepancies between the simulated results and the actual performance of a physically realized antenna system. These discrepancies can arise from various factors, including inaccuracies in material properties, simplifications in the modeling process, or unforeseen environmental factors that are difficult to account for in simulations. To mitigate these limitations, it is crucial to validate the simulation results through physical prototyping and field testing. While computer simulations offer a valuable starting point and provide insights into the antenna's behavior, they should be complemented by empirical data obtained from real-world experiments. This iterative process of simulation, prototyping, and testing can help refine the design and calibrate the computational models, leading to more accurate and reliable results.

Another aspect that warrants further investigation is the exploration of alternative materials and fabrication techniques for the ultrawideband Vivaldi active phased array antenna. While the current design utilizes conventional materials and manufacturing processes, advances in material science and additive manufacturing technologies may offer new opportunities for enhancing the antenna's performance, reducing costs, or improving its environmental sustainability.

For instance, the use of advanced composite materials or metamaterials could potentially improve the antenna's bandwidth, efficiency, or radiation characteristics. Additionally, additive manufacturing techniques, such as 3D printing, could enable the production of complex antenna

geometries with increased precision and reproducibility, while minimizing material waste and reducing the environmental impact of traditional manufacturing processes.

Furthermore, the integration of the ultrawideband Vivaldi active phased array antenna with other technologies and applications presents an exciting avenue for future research. For example, the antenna could be combined with emerging Internet of Things (IoT) technologies, enabling seamless connectivity and data transmission for various smart devices and sensors deployed in ecological monitoring scenarios.

Additionally, the antenna system could be adapted for use in other domains, such as remote sensing, environmental monitoring, or even biomedical applications, where reliable and high-bandwidth data transmission is crucial [13-16]. The integration of the antenna with cyberphysical systems [17,18] and biosensors for remote monitoring of biosignals is an area of particular interest, as it could enable real-time monitoring of various biological parameters in remote or challenging environments [19-25].

To facilitate these future research directions, it is essential to foster interdisciplinary collaborations among researchers from various fields, including antenna design, material science, additive manufacturing, IoT technologies, and biomedical engineering. By bringing together diverse expertise and perspectives, innovative solutions and synergistic advancements can be achieved, further enhancing the capabilities and applications of the ultrawideband Vivaldi active phased array antenna.

The computer simulation approach has proven to be a valuable tool in the development of advanced antenna technologies, such as the ultrawideband Vivaldi active phased array antenna. However, it is important to recognize its limitations and address them through physical prototyping, field testing, and the exploration of alternative materials and fabrication techniques. Additionally, the integration of the antenna system with emerging technologies and its adaptation for diverse applications present exciting opportunities for future research. By embracing interdisciplinary collaborations and fostering innovation, the full potential of this technology can be unlocked, contributing to advancements in ecological monitoring, drone video broadcasting, and various other domains that rely on reliable and high-performance data transmission.

Conclusion

The present study has demonstrated the significant advantages of employing computer simulations in the development of advanced technologies, exemplified by the ultrawideband Vivaldi active phased array antenna. This approach offers substantial benefits over traditional methods, including reduced costs, enhanced environmental sustainability, and improved control over experimental conditions. Through comprehensive computer simulations, we have successfully designed and optimized an ultrawideband Vivaldi active phased array antenna capable of operating across multiple frequency bands, including 1.2 GHz, 2.4 GHz, 5.6 GHz, and 5.8 GHz. This versatile antenna system is well-suited for applications in ecological monitoring and drone video broadcasting, surpassing the limitations of traditional omnidirectional antennas.

One of the key advantages of computer simulations is the cost-effectiveness compared to physical prototyping and field experiments. By utilizing sophisticated computational models and simulation tools, we can explore various design configurations, optimize performance parameters, and evaluate the antenna's behavior in diverse environmental conditions without incurring the substantial expenses associated with fabricating multiple physical prototypes or conducting extensive field trials. Moreover, computer simulations contribute to environmental sustainability by minimizing the need for physical experiments and reducing the ecological footprint associated with traditional development processes. This aligns with the overarching goal of ecological monitoring, as the simulations themselves have a negligible impact on the environment, ensuring a greener and more responsible approach to technological advancements.

The flexibility and control offered by computer simulations are unparalleled. Unlike physical experiments, where variables are often challenging to isolate and control, simulations enable

precise manipulation of various parameters, such as environmental conditions, interference sources, and operational scenarios eliminating potential health risks. This level of control facilitates a deeper understanding of the antenna's performance and enables the identification of optimal configurations tailored to specific applications.

The proposed ultrawideband Vivaldi active phased array antenna offers significant advantages over traditional omnidirectional antennas. By covering multiple frequency bands simultaneously, it enables efficient and reliable video transmission for drone applications, enhancing the effectiveness of ecological monitoring and broadcasting operations.

Additionally, the phased array configuration allows for electronic beam steering and narrowing, resulting in increased communication range and reduced electromagnetic interference with other devices. This adaptability ensures a robust and stable communication link with drones, even as they navigate through various environments, while minimizing potential disruptions to other systems or receivers.

In conclusion, the computer simulation approach employed in this study has proven to be a highly effective and sustainable method for the development of advanced antenna technologies like the ultrawideband Vivaldi active phased array antenna. This achievement not only demonstrates the technical capabilities of computer simulations but also highlights their potential for fostering innovation while promoting environmental responsibility and societal well-being.

Declaration on Generative AI

The authors have not employed any Generative AI tools.

References

[1] Díaz-Delgado, R., & Mücher, S. (Eds.). Drones for Biodiversity Conservation and Ecological Monitoring. MDPI. 2019 Dec 18. doi: 10.3390/drones3020047.

[2] Moreta, J., Moreno, H., Caicedo, F. (2022). Real-Time Video Transmission and Communication System via Drones over Long Distances. In: Garcia, M.V., Fernández-Peña, F., Gordón-Gallegos, C. (eds) Advances and Applications in Computer Science, Electronics, and Industrial Engineering. CSEI 2021. Lecture Notes in Networks and Systems, vol 433. Springer, Cham.

[3] Vergouw, B., Nagel, H., Bondt, G., Custers, B. (2016). Drone Technology: Types, Payloads, Applications, Frequency Spectrum Issues and Future Developments. In: Custers, B. (eds) The Future of Drone Use. Information Technology and Law Series, vol 27. T.M.C. Asser Press, The Hague. doi: 10.1007/978-94-6265-132-6_2.

[4] Ghimire, J., Diba, F. D., Kim, J. H., & Choi, D. Y. (2021). Vivaldi antenna arrays feed by frequency-independent phase Shifter for high directivity and gain used in microwave sensing and communication applications. Sensors, 21(18), 6091. doi: 10.3390/s21186091.

[5] Hatami, A., Saee Arezomand, A. & Zarrabi, F.B. (2020). Phase center controlling in Vivaldi antenna: review and development of the story. J Comput Electron 19, 736–749.

[6] Langley, J. D. S., Hall, P. S. Newham, P. (1996). Balanced antipodal Vivaldi antenna for wide bandwidth phased arrays. IEE Proceedings-Microwaves, Antennas and Propagation, 143(2), 97-102. doi: 10.1049/ip-map:19960260.

[7] Mailloux, R.J. Phased array antenna handbook, 2nd ed., Artech house, 2017.

[8] Balanis, C.A. Antenna Theory, Analysis and Design, Chapter 2, sec 2.3-2.6, Wiley.

[9] Makarov, Sergey N. Antenna and Em Modeling in MATLAB. Chapter3, Sec 3.4 3.8., Wiley Inter-Science.

[10] Vasiliadis, T.G., A.G. Dimitriou and G.D. Sergiadis, "A novel technique for the approximation of 3-D antenna radiation patterns," in IEEE Transactions on Antennas and Propagation, July 2005, vol. 53, no. 7: pp. 2212-2219.

[11] Leonor N.R., R.F.S. Caldeirinha, M.G. Sanchez and T.R. Fernandes, "A Three-Dimensional Directive Antenna Pattern Interpolation Method" in IEEE Antennas and Wireless Propagation Letters, 2016, vol. 15, pp. 881-884. doi: 10.1109/LAWP.2015.2478962.
[12] Pandey, G. K., Singh, H. S., Bharti, P. K., Pandey, A., & Meshram, M. K. (2015). High gain Vivaldi antenna for radar and microwave imaging applications. International Journal of Signal Processing Systems, 3(1), 35-39. doi: 10.12720/ijsps.3.1.35-39.
[13] Khvostivska L., Khvostivskyi M., Dediv I., Yatskiv V., Palaniza Y. Method, Algorithm and Computer Tool for Synphase Detection of Radio Signals in Telecommunication Networks with Noises. Proceedings of the 1st International Workshop on Computer Information Technologies in Industry 4.0 (CITI 2023). CEUR Workshop Proceedings. Ternopil, Ukraine, June 14-16, 2023. pp.173-180. ISSN 1613-0073.
[14] Lytvynenko I. Methods of Processing Cyclic Signals in Automated Cardiodiagnostic Complexes. Proceedings of the 1st International Workshop on Information-Communication Technologies & Embedded Systems (ICTES 2019) Mykolaiv, Ukraine, 2019. pp. 116-127.
[15] Romaniv, S.V., Palaniza, Y.B., Vakulenko, D.V., Galaychuk, I.Y. "The method of using fractal analysis for metastatic nodules diagnostics on computer tomographic images of lungs" Horizons in Cancer Research, March 30, 2023, v. 85, pp. 231–247.
[16] Palianytsia, Y, Vasyl, D, Khvostivska, L. “Modeling of Phased Array Antenna for Data Transmission in Urban Environment.” Proceedings of the 3rd International Workshop on Information Technologies: Theoretical and Applied Problems, 22-24 November 2023, Ternopil, Ukraine, edited by Lytvynenko I.V. and Lupenko S.A., ITTAP-2023, 2023, pp. 370-381.
[17] Buketov, A.; Maruschak, P.; Sapronov, O.; Zinchenko, D.; Yatsyuk, V.; Panin, S. Enhancing Performance Characteristics of Equipment of Sea and River Transport by Using Epoxy Composites. Transport 2016, 31, 333–342.
[18] Maruschak, P. O., Panin, S. V., Zakiev, I. M., Poltaranin, M. A., Sotnikov, A. L. (2016). Scale levels of damage to the raceway of a spherical roller bearing. In Engineering Failure Analysis (Vol. 59, pp. 69–78). https://doi.org/10.1016/j.engfailanal.2015.11.019
[19] Martsenyuk, V., Klos-Witkowska, A., & Sverstiuk, A. (2020). Stability Investigation of Biosensor Model Based on Finite Lattice Difference Equations. In Springer Proceedings in Mathematics & Statistics (pp. 297–321). Springer International Publishing.
[20] Martsenyuk, V., Sverstiuk, A., & Gvozdetska, I. S. (2019). Using Differential Equations with Time Delay on a Hexagonal Lattice for Modeling Immunosensors. In Cybernetics and Systems Analysis (Vol. 55, Issue 4, pp. 625–637). Springer Science and Business Media LLC.
[21] Martsenyuk, V. P., Andrushchak, I. Ye., Zinko, P. N., & Sverstiuk, A. S. (2018). On Application of Latticed Differential Equations with a Delay for Immunosensor Modeling. In Journal of Automation and Information Sciences (Vol. 50, Issue 6, pp. 55–65). Begell House.
[22] Sverstiuk A.S. Research of global attractability of solutions and stability of the immunosensor model using difference equations on the hexagonal lattice (2019) Innovative Biosystems and Bioengineering, 3 (1), pp. 17 – 26. DOI: 10.20535/ibb.2019.3.1.157644. +3
[23] Martsenyuk V.P., Sverstiuk A.S., Andrushchak I.Ye. Approach to the study of global asymptotic stability of lattice differential equations with delay for modeling of immunosensors (2019) Journal of Automation and Information Sciences, 51 (2), pp. 58 – 71. DOI: 10.1615/jautomatinfscien.v51.i2.70. +3
[24] Franchevska, H., M. Khvostivskyi, V. Dozorskyi, E. Yavorska, O. Zastavnyy. The Method and Algorithm for Detecting the Fetal ECG Signal in the Presence of Interference. 1st International Workshop on Computer Information Technologies in Industry 4.0 (CITI 2023). Ternopil 14 -16 June 2023. Vol. 3468, P. 263-272. ISSN 1613-0073.
[25] Khvostivskyy M., Osukhivska H., Khvostivska L., Lobur T., Velychko D., Hovorushchenko T., Lupenko S. Mathematical modelling of daily computer network traffic. Proceedings of the 1st International Workshop on Information Technologies: Theoretical and Applied Problems 2021 (ITTAP 2021). Ternopil, Ukraine. November 16-18, 2021. Vol. 3039, P.107-111. ISSN 1613-0073.